Contents lists available at ScienceDirect

Chemical Engineering Research and Design

journal homepage: www.elsevier.com/locate/cherd

Liquid–liquid centrifugal separation — New equipment for optical (photographic) evaluation at laboratory scale

*Armin Eggert, Stephan Sibirtsev, David Menne, Andreas Jupke**

AVT — Fluid Process Engineering, RWTH Aachen University, Aachen, Germany

ARTICLE INFO

Article history:
Received 26 June 2017
Accepted 5 September 2017
Available online 12 September 2017

Keywords:
Centrifugal liquid–liquid separation
Batch settling cell
Sedimentation
Enhanced force field
Coalescence
Dispersion number

ABSTRACT

Since liquid–liquid separation techniques are applied in chemical process industry, research and development received a strong level of attention. Thus, liquid–liquid separation behavior in gravity equipment – e.g., in settling tanks – especially sedimentation and coalescence are investigated in detail. However, for liquid–liquid separation in centrifugal equipment – e.g., tube centrifuges – only superficial knowledge and less detailed investigations are given in open literature. This work focuses on the development of a new laboratory equipment for optical (photographic) evaluation of the centrifugal liquid–liquid separation processes. A new **s**tirred **c**entrifugal **b**atch **s**ettling **c**ell (SCBSC) utilizing a rotor–rotor/stator concept, experimental setup and method as well as analytical procedures are presented and discussed. Furthermore, results of mixing and separation process within the SCBSC are shown. The centrifugal force field thereby affects the required differential rotation speed for the dispersion process. The evaluation of the separation process is presented and discussed considering sedimentation and coalescence curves exemplary for two liquid–liquid systems. In the course of this, a comparison between gravitational and centrifugal separation was successful. Finally, the separation behavior is described by a dimensionless dispersion number.

1. Introduction

The separation of a mixture consisting of two immiscible liquids into two coherent phases is an important task in (petro-) chemical, biotechnological, pharmaceutical as well as in food industry. For example, industrial applications, such as in extraction processes, multi-phase reaction systems, (offshore) oil exploration or hetero azeotrope distillation, frequently require liquid–liquid separation techniques. Separation behavior and consequently equipment performance depends on chemo-physical parameters, such as density difference between the two phases, viscosity of the continuous phase, dispersed phase fraction and surface tension. Since liquid–liquid separation is challenging, various separation techniques were developed to counter different separation challenges. Thus, a broad range of techniques and equipment is available for custom-made liquid–liquid separation process engineering. Reliable methods for selection of a suitable separation technique as well as calculation and design of equipment and performance are of particular interest. Therefore, separation phenomena have received a strong attention in research and development in the last decades. In order to obtain better separation efficiency, an increase of the force field by centrifugal rotation is an attractive technique. Thus, the centrifugal acceleration and the resulting mass force can be increased up to 10^6 times higher compare to the gravity force field. Literature surveys of different types of centrifugal equipment, separators and extractors, can be found in (Beveridge, 2000; Gebauer et al., 1982; Schaflinger, 1990; Simon, 1982; van Kemenade et al., 2014). Schaflinger and Beveridge summarizes various types of centrifugal separators (centrifuges, decanters and cyclones) for different types of multi-phase mixtures (Beveridge, 2000; Schaflinger, 1990). Gebauer et al. gives a schematic classification for centrifugal separation and extraction equipment (Gebauer et al., 1982).

* *Corresponding author at*: Forckenbeckstraße 51, 52074 Aachen, Germany.
E-mail addresses: Armin.Eggert@avt.rwth-aachen.de (A. Eggert), Stephan.Sibirtsev@avt.rwth-aachen.de (S. Sibirtsev), David.Menne@rwth-aachen.de (D. Menne), Andreas.jupke@avt.rwth-aachen.de (A. Jupke).
http://dx.doi.org/10.1016/j.cherd.2017.09.005

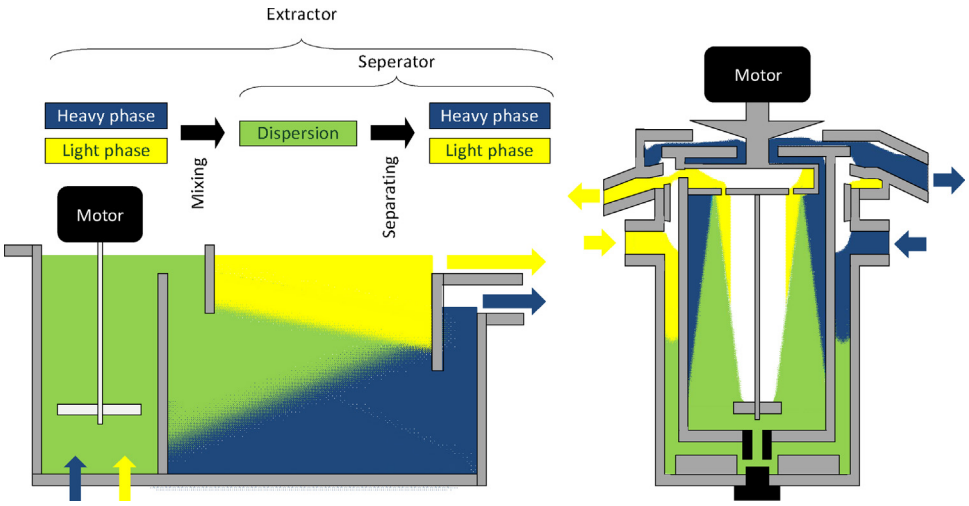

Fig. 1 – Analogies of mixer settler units for extraction processes in the gravitational field (left) and in the centrifugal field (right). Blue (heavy phase) and yellow (light phase) arrows visualizes the entrance and outlet of the coherent liquids, green the homogenous mixed liquid–liquid dispersion. The separation process in the settling tank and in the rotor zone is indicated by the wedge-shaped dispersion band. (For interpretation of the references to color in this figure legend, the reader is referred to the web version of this article.)

Further Gebauer et al. distinguishes between continuous mixer-settler devices and differential contactors for extraction processes (Gebauer et al., 1982). The first group enables mixing and complete separation of two liquids in each equilibrium stage, the second group operates with non-discrete counter current flow which enables more equilibrium stages in one device. The comparison of classic continuous mixer-settler (MS) in the gravitational field (left) and the centrifugal field is shown in Fig. 1. One of the most commonly used continuous centrifugal extractors with liquid–liquid separation in the rotor zone is the annular centrifugal contactor (ACC), or synonymously used annular centrifugal extractor (ACE) (Vedantam and Joshi, 2006). In the annular gab between the housing and the rotor of the ACC, which represents the mixing part of the extractor, the mixing process takes place. In the rotor zone, which represents the settling part of the extractor, the separation occurs. Thus, two coherent liquid phases enter and leave the centrifugal device. The ACC was developed by Bernstein in 1973 and experimentally investigated in detail by Leonard et al. and further researches in several experimental works (Arafat et al., 2001; Bernstein et al., 1973, 1987; Birdwell et al., 2006; Cao et al., 2013; Duan et al., 2005; Duan and Cao, 2015; Kadam et al., 2008, 2009; Klasson et al., 2005; Leonard, 1988; Leonard et al., 1997, 2001, 2006; Mandal et al., 2015; Meikrantz et al., 2001, 2005; Svn Ayyappa et al., 2014; Webster et al., 1967). In all these works no investigations considering detached mixing and separation was performed. However, there are experimental based further developments of the classic ACC (Duan et al., 2009; Meikrantz et al., 2002; Rivalier et al., 2004). The most comprehensive and detailed research of centrifugal extraction equipment was carried out in the collaborative research center 153 “reaction and mass transfer technique for dispersed two-phase systems”. In this collaborative research center, several researches focused on the drop formation and drop motion process within the Podbielniak differential centrifugal extractor (ReinholdSchilp_1982_Fluiddynamik in Zentrifugal-Extraktoren I; Otillinger, 1988; Schilp, 1983; Schilp and Blaß, 1982, 1983; Stölting et al., 1979; Stölting, 1979; Stölting and Blaß, 1978). However, for centrifugal liquid–liquid separation only few detailed investigations for sedimentation and even less for coalescence phenomena are given in literature (Jammoal and Lee, 2015; Otillinger, 1988). Other researchers quantified separation kinetics and efficiency for centrifugal oil–water separator with plate pack internals (Plat, 1994) or for stable oil–water emulsions in tube centrifuges (Cambiella et al., 2006; Krebs et al., 2012). From the state of the art it is evident that there are no established studies, which present a clear understanding of the flow dynamics, such as sedimentation and coalescence of dispersed droplet swarms within centrifugal force field. Despite these facts, few authors deal with modeling and CFD simulation of the rotor zone, neglecting that a validation and quantification of the simulation is challenging (Li et al., 2012; Padial-Collins et al., 2006; Patra et al., 2013; Vedantam et al., 2012; Wardle et al., 2009). Thus, the simulation is only being discussed qualitatively with basic physical knowledge and experience from gravitational separator. However, from the state of the art the simulated results seem unsuitable for reliable equipment design and performance prediction. Rather a clear request for investigation of the rotor zone was formulated in (Vedantam and Joshi, 2006). Thus, a gab in understanding certain hydrodynamic effects and their influence on the liquid–liquid separation kinetic within centrifugal equipment of various scales and operational modes is identified. Therefore, a detailed study on the flow dynamics in the rotor regions becomes imperative. Thus, phase separation should be investigated within the centrifugal field. To understand the influence of higher acceleration on phase separation phenomena optical measurements of the rotor zone is implemented in batch experiments. A new cylindrical equipment applied for experimental investigations and graphical analyses of the experiments will be presented.

The gravitational settler as illustrates in Fig. 1 is one of the frequently used devices in liquid–liquid separation techniques, which gives a good example of how the liquid–liquid separation behavior can be determined. The separation of two immiscible liquids is characterized by droplet sedimentation, droplet–droplet coalescence, droplet–interface coalescence and the overall separation time. Henschke developed a nowadays well-established laboratory scale experimental method for the liquid–liquid separation using a standardized stirred batch settling cell. Combined with a model-based approach the settler can be designed based on laboratory scale data (Henschke, 1995). Schematic sedimentation and coalescence curves are shown in Fig. 2 and are described in detail in literature. Both, sedimentation and coalescence, can be described mathematically by detailed single drop and droplet swarm models (Henschke, 1995). For model parameter determination, droplet Sauter mean diameter and coalescence time as well as experimental data from laboratory scale batch separation experiments are necessary. For a better comparability of the gravitational and centrifugal separation progress the experiments will be presented in a normalized way. Normalization of the separation progress is determined by the percentage of the separation progress with regard to the overall separation, Eqs. (1) and (2).

$$h\% = \frac{h = f(t)}{h_0} \tag{1}$$

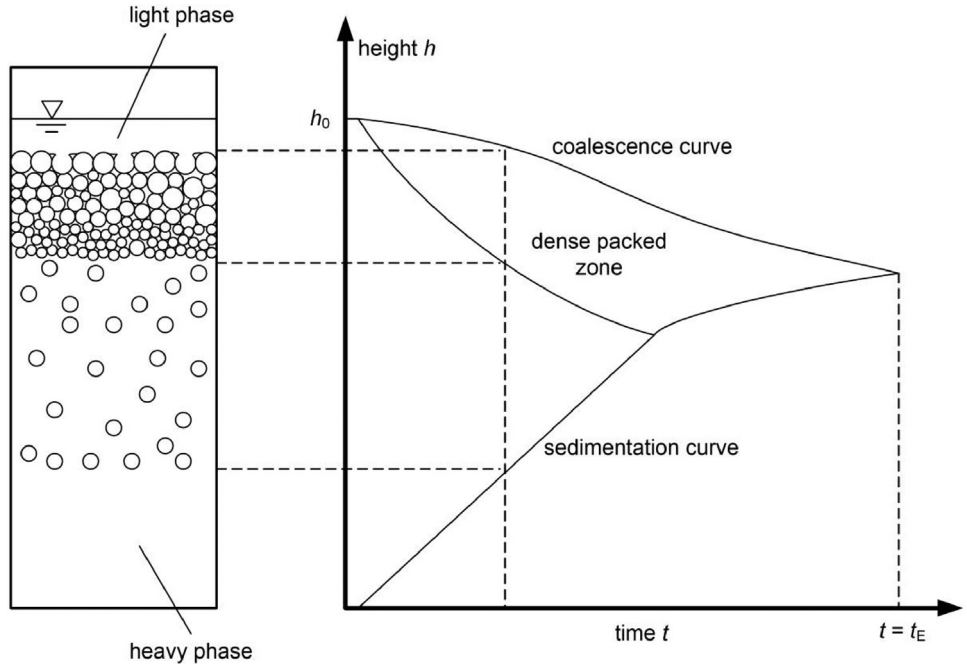

Fig. 2 – Schematic illustration of the liquid–liquid separation process of batch experimental investigations within the gravitational field as proposed by Henschke (1995). Separation progress (sedimentation and coalescence) of the lighter dispersed phase is characterized by the sedimentation curve, coalescence curve and overall separations time t_E.

Table 1 – Physical properties of saturated liquid–liquid systems (Henschke, 1995).

System		ρ (kg/m^3)	η (mPa s)	σ (mN/m)	Phase state
1	Water	987	1.463	1.75	Continuous
	n-Butanol	846	3.32		Dispersed
2	Water	999	1.323	3.8	Continuous
	Cyclohexanone	953	2.31		Dispersed

$$t\% = \frac{t = f(x)}{t_E} \tag{2}$$

For centrifugal separators design and performance calculation is still based on simplified models and expert knowledge or expensive and time-consuming pilot-plat experiments (Brunner, 1985; Hemfort, 1983; Rousselet Robatel). Furthermore, these kinds of studies are barely reported in the available literature. However, one empirical correlation to predict the separation efficiency depending on the centrifugal force field, is given in its most general form by Leonard, Eq. (3), (Leonard et al., 1981; Leonard, 1995).

$$N_{Di} = \frac{1}{t} \cdot \sqrt{\frac{\Delta Z}{a}} = \frac{1}{t} \cdot \sqrt{\frac{r_o - r_i}{a}} \tag{3}$$

$$a = \bar{r} \cdot \omega^2 = \bar{r} \cdot (2\pi n)^2 \tag{4}$$

$$\bar{r} = \frac{2 \cdot (r_o^3 - r_i^3)}{3 \cdot (r_o^2 - r_i^2)} \tag{5}$$

In this context N_{Di} is called the "Dispersion Number" and is primarily proposed for dispersion characterization. Furthermore, a is the acceleration of the dispersed system as defined in Eq. (4), t is the characteristic average residence time of the dispersion band as defined in Eq. (5) and ΔZ is the thickness of the dispersion band in direction of acceleration, given bei the difference of the outer radius r_o and the inner radius r_i. This correlation was established and experimentally investigated by an integral, black-box investigation of the liquid–liquid flow pattern in the rotor zone of an ACC (Leonard, 1995). For a batch system, as given in standardized settling tests, t_i is the overall separation time and for a continuous settler operation t_i is defined as the quotient of dispersion volume V in the settling zone and the volumetric flow rate q, Eq. (6).

$$t_r = \frac{V}{q} \tag{6}$$

2. Material and methods

2.1. Chemical system

For experiments with the SCBSC, *n*-butanol/water and cyclohexanone/water as liquid–liquid systems were chosen. The physical properties are summarized in Table 1. The organic phase *n*-butanol was provided by Merck, Darmstadt, Germany, with a purity of 99%, cyclohexanone from CarlRoth, München, Germany, with a purity of 98%. The aqueous phase was deionized and distillated in a MonoDest3000 distillery from Lenz Glas Instrumente, Wertheim, Germany. Furthermore for water conditioning sodium chloride (NaCl), with purity of 99%, was provided by Merck, Darmstadt, Germany.

2.2. Experimental set-up

To observe the separation of disperse liquid–liquid systems in centrifugal force field a new laboratory equipment is required. Thus, and for a high level of reproducibility a (standardized) **s**tirred **c**entrifugal **b**atch **s**ettling **c**ell (SCBSC) at laboratory scale was developed and applied for patent (Eggert et al., 2016a). Furthermore, the setup was improved and can be utilized now as a centrifugal reactor concept for fast

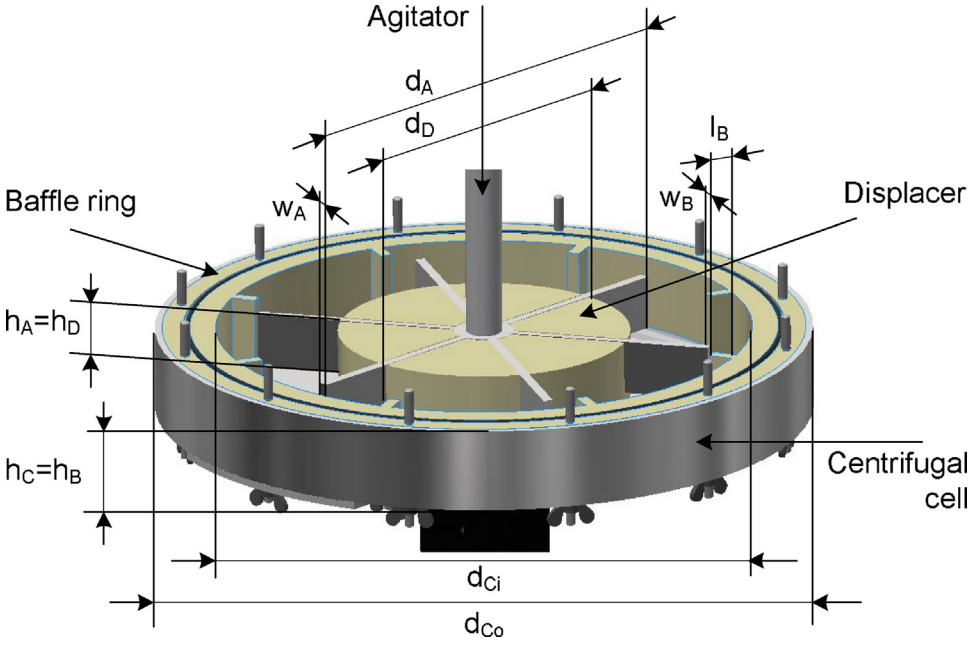

Fig. 3 – Illustration of the rotor–rotor/stator concept, CAD-Model of the SCBSC, dimensions given in Table 2. Key elements are the centrifugal cell with a baffle ring and the agitator with a displacer.

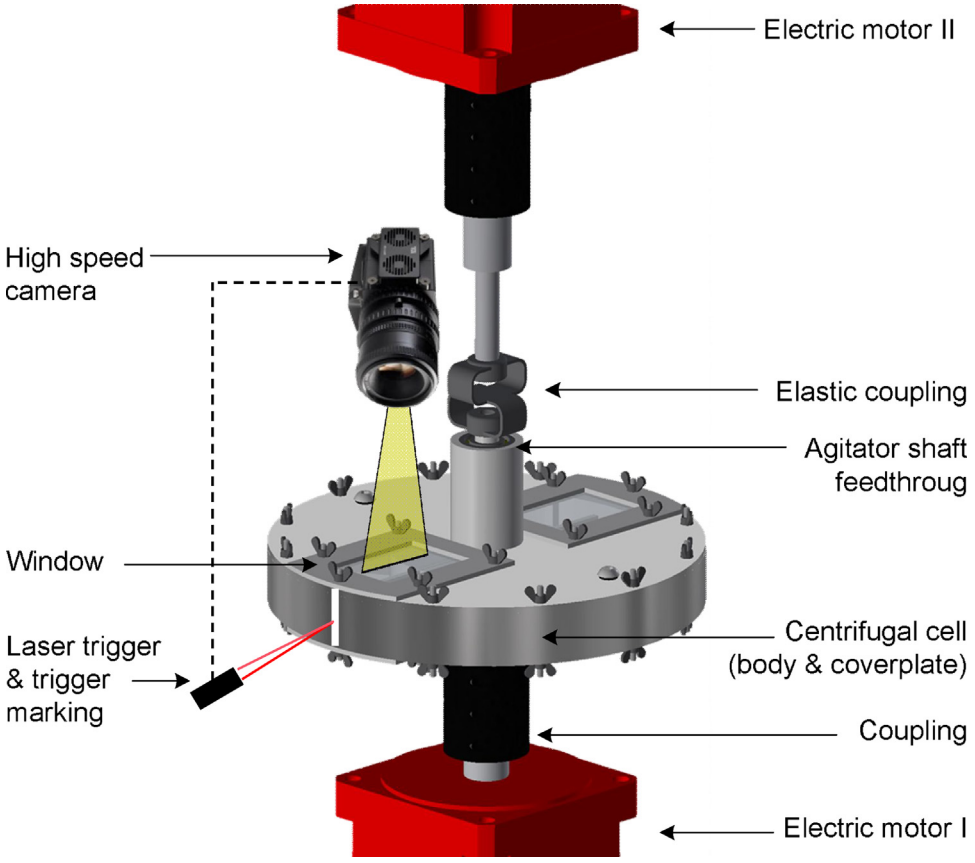

Fig. 4 – Illustration of the experimental setup of the SCBSC with electric motor arrangement and high-speed camera system.

mixing and separation, minimizing contact times for reactions, in small closed batch vessels (not shown here) (Eggert et al., 2016b). For chemical resistance all components of the SCBSC are made out of stainless steel (1.4401), polypropylene (PP), polytetrafluorethylene (PTFE) and glass. To realize the mixing and separation process within one device a switchable rotor–rotor/stator principle is applied. To realize the rotor–rotor/stator functionality the SCBSC is constructed in two parts, a closed hollow-cylindrical body, the rotor, and an agitator, the rotor/stator. The SCBSC as well as the experimental setup is shown in Figs. 3 and 4. Furthermore, all dimensions for the SCBSC are given in Table 2.

The hollow-cylindrical cell has an outer diameter of 280 mm and a height of 30 mm. Due to a coaxial inlay, the baffle ring, the interior space of the SCBSC is 220 mm. With eight baffles, 10 mm in depth and 4 mm in width, the baffle ring has two essential functions. First, the enhancement of the turbulence while mixing and second to improve the accel-

Table 2 – Dimensions of SCBSC CAD-Model, Fig. 3.

Component	Dimension	Symbol	Value (mm)
Stirrer	Diameter	d_A	200
	Height	h_A	28
	Width	w_A	4
Displacer	Diameter	d_D	80/120
	Height	$h_D = h_A$	28
Centrifugal cell	Diameter	d_{Co}	280
	Height	h_C	30
Baffle ring	Diameter	d_{Bi}	220
	Height	h_B	30
	Width	w_B	5
	Length	l_B	10

eration of the liquid–liquid system in the separation process. To observe the separation process two glass windows with a size of 70 × 50 mm are mounted on the axial front surfaces of the SCBSC. On the cover plate, a sealed feedthrough for the agitator shaft is placed centrically. The agitator consists of a six-blade paddle stirrer with a size of 22 mm in height and 190 mm in diameter, fixed on a shaft and a displacer, which has two major functions. First, to relocate the separation process to higher centrifugal forces and second to limit the total free liquid volume of the centrifugal cell from 950 ml to 700 ml without applying of a gas pocket. Thereby, no gas is mixed in the liquid–liquid disperse system during the mixing. The displacer can be varied from 80 mm to 120 mm in diameter. Both, the hollow-cylindrical body as well as the agitator are coupled and powered by separate servo electric motors (type: CMPZ 80 M, 11 kW, 400 V, 50 Hz, up to 6000 rpm, supplied by SEW-EURODRIVE GmbH & CoKG, Bruchsal, Germany) as shown in Fig. 4. These motors enable rotations in both directions. To regulate the direction and rotation speed, manually or via control software, the motors are connected to frequency converters (type: MOVIDRIVE® MDX60B, supplied by SEW-EURODRIVE GmbH & CoKG, Bruchsal, Germany). For the optical observation a high speed video camera (type: Os4S1-C-O4, 8 GB DDR working storage, 512 GB SSD intern storage, 1024 × 1024 pixels, 6.000 frames per second (fps), supplied by Imaging Solutions GmbH, Eningen, Germany) with a camera objective (type: LM16HC, 1″ 16 mm/F1.4, supplied by Kowa Optimed Deutschland GmbH, Duesseldorf, Germany) is used. The camera is installed perpendicular to the centrifugal cell rotation axis. Thus, the camera is focusing on the centrifugal cell front surface and glass windows. The camera is triggered by a laser light barrier and a trigger marker on the cylinder wall. Camera and recording settings are controlled via Ethernet linkage and the Motion Studio PC software (v. 2.12.05). For a sufficient lighting performance, required for short exposure times, a 500 W light emitting diode (LED) is used. The 500 W LED is powered by a direct current (DC) laboratory power supply (type: PS 8360-10 T, 0…360 V, 0…10 A, up to 1000 W, supplied by Elektro-Automatik GmbH & Co. KG, Viersen, Germany). For temperature control the experimental equipment is located in a housing, which is vented by a fan heater. The fan heater is controlled by a PID controller.

2.3. *Experimental preparation*

Prior to the experimental investigations the liquid phase systems were mutually saturated. According to experimental conditions, the temperature was set to 25 °C. The volumetric ratio for saturation was 1:1 (V_{org}:V_{aq}). The water was conditioned with ions by addition of 5.0 g/l NaCl. The experimental equipment was disassembled completely and all components were first rinsed with deionized, distilled water, followed by acetone and finally with deionized, distilled water again. All components were dried at 40 °C for 12 h before the cell was assembled. After assembling, the settling cell was filled and installed in the test stand.

2.4. *Experimental method*

The experimental method is characterized by consecutively alternating process steps of mixing and separation within the centrifugal force field. For better illustration an animated video of the SCBSC is given in Video 1.

In order to generate the centrifugal force field, the centrifugal cell and the agitator are powered synchronously in direction and at the same basic rotational speed. Thereby, an orientation of the liquid phases in direction of the centrifugal acceleration takes place: The light phase is located at the displacer and the heavy phase is located at the baffle ring. The annular liquid layers and the phase boundary are observed vertically through the glass window. To generate the dispersion inside the SCBSC a differential rotation speed between the centrifugal cell and the agitator is applied. For this purpose, the rotational speed of the agitator is changed while the centrifugal cell is kept on basic rotational speed. Thus, the differential rotational speed Δn as given in Eq. (7) is defined as the difference of rotational speed of the centrifugal cell n_c and the agitator n_s.

$$\Delta n = n_c - n_s \tag{7}$$

The differential rotational speed introduces a power input into the liquid–liquid system. This power input causes turbulences which result in droplet formation. After the liquid–liquid dispersion is formed, the agitator is switched back to basic rotation speed in 20 ms, thus the separation process is initiated as shown in Fig. 5. The relative motion between the baffle ring and the stirrer is interrupted while the synchronized rotation. Opposite to the mixing the turbulence field within the centrifugal cell collapses as no further power input is initiated. Consequently, the liquid phases are now accelerated only in radial direction to the axis of the rotation. The heavy phase flows outward and accumulates at the inner wall of the baffle ring. The light phase flows inward and accumulates at the outer wall of the displacer. At the same time as the phase separation process starts the high speed camera system starts recording the process.

2.5. *Analytical method*

The analytical method is based on the optical observation of the liquid–liquid separation during the centrifugation process as shown in Fig. 6. Due to a trigger signal one picture per revolution is recorded. All images are stored on an internal SSD card of the camera. The images are analyzed offline by picture evaluation considering the region of interest to follow a radial trajectory to the axis of rotation. The evaluation is simplified by a millimeter raster in cylindrical coordinates as shown in Fig. 5, which was placed on the window. The separation progress is quantified by path-time coordinates. Each path coordinate includes a value for the sedimentation and

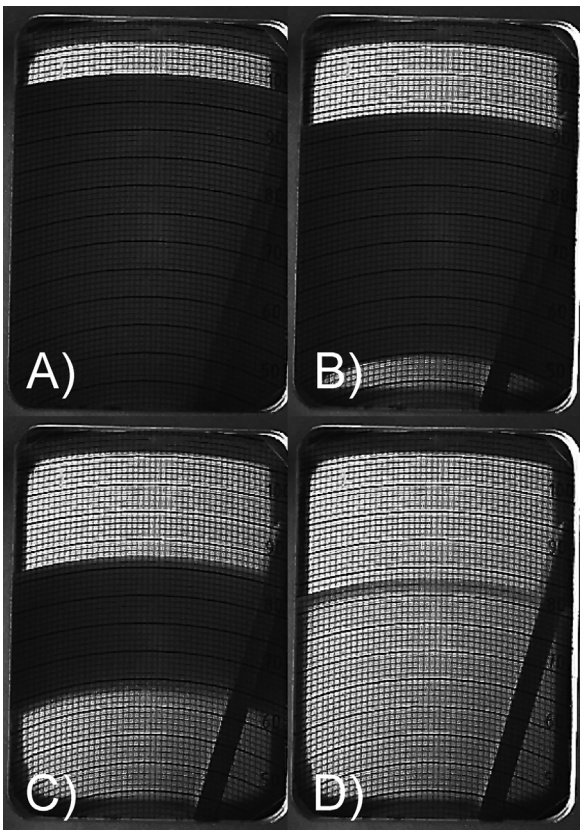

Fig. 5 – Separation process for *n*-butanol/water-system with volumetric ratio of V_{org}:V_{aq} 1:1 and displacer r = 60 mm after mixing with Δn = 500 rpm. Basic rotational speed is set to n_c = 900 rpm. (A–C) show the separation progress for different times; (A) t = 150 ms, (B) t = 300 ms, (C) t = 450 ms and (D) t = 900 ms.

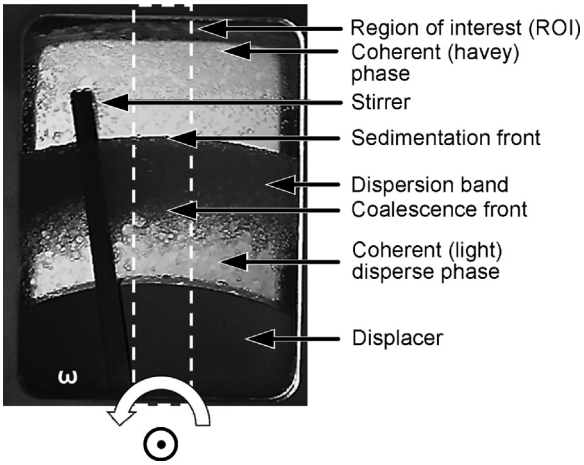

Fig. 6 – Illustration of the photographic evaluation in the region of interest (ROI). Image shows top view of one SCBSC window, agitator elements (displacer and stirrer), both coherent liquids and the dispersion band, demarcated by sedimentation and coalescence front, can be seen clearly.

coalescence progress. This way, the characteristic separation curves, sedimentation and coalescence, are determined.

3. Results and discussion

The required differential rotation Δn for the formation of the dispersion depends strongly on the basic rotation n_c. The mixing process for various combinations of centrifugal cell and agitator rotational speed is shown in Figs. 7 and 8 (a more detailed example is given in the supplementary). In Fig. 7A the turbulence field induced by Δn = 50 rpm is insufficient to overcome the centrifugal force field of n_c = 900 rpm. With an increase of the differential rotation in Fig. 7A–E a stronger dispersion formation within the centrifugal cell and over the centrifugal cell radius takes place. Thus, a marked increase of the dispersion band thickness is determined. The same tendency can also be observed for a negative Δn as shown in Fig. 8. For a constant Δn and an increased basic rotation n_c the dispersion band thickness decreases. Since the induced turbulences enable disperse phase transport contrary to the buoyance force ($F_b = m \cdot a = V_d \cdot \Delta\rho \cdot (2\pi n_c)^2 \cdot r$) a higher basic rotation requires a higher differential rotation Δn. Thus, with an increase in the basic rotational speed a further increase in the differential rotational speed is needed to overcome the centrifugal acceleration.

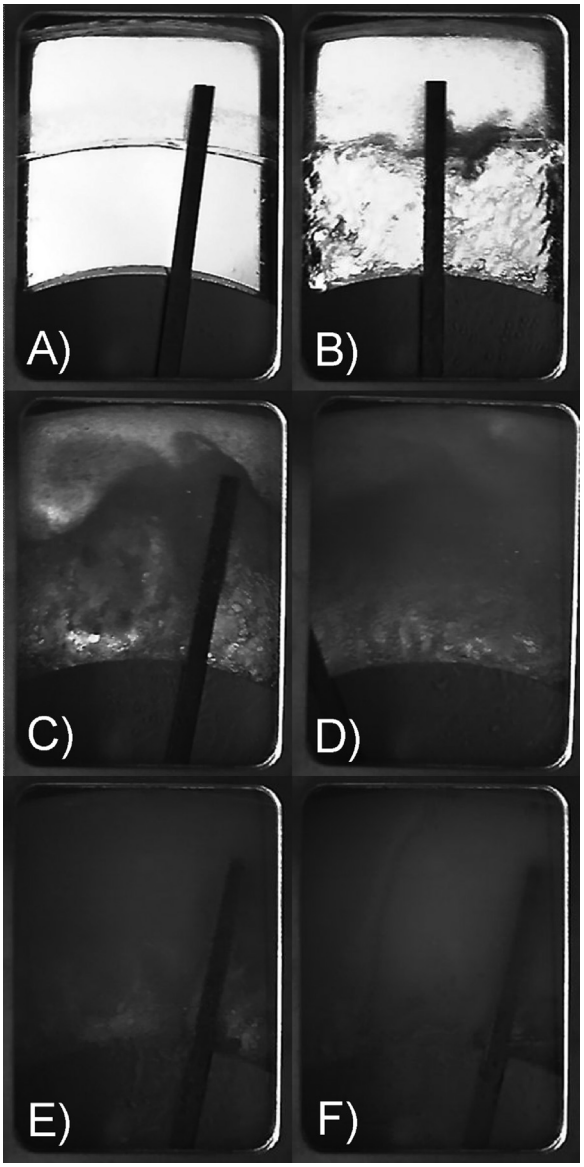

Fig. 7 – Illustration of the mixing process with volumetric ratio of V_{org}:V_{aq} 1:1 and displacer r = 60 mm. Basic rotational speed constant at n_c = 900 rpm. Rotational speed of agitator is increased stepwise with n_s = 50 rpm. Differential speed: (A) Δn = 50 rpm, (B) Δn = 100 rpm, (C) Δn = 150 rpm, D) Δn = 200 rpm, (E) Δn = 250 rpm and (F) Δn = 300 rpm.

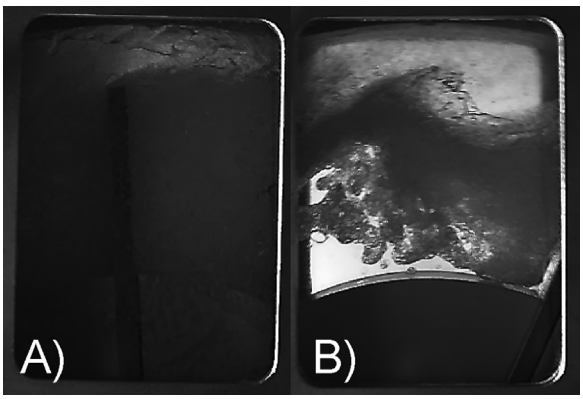

Fig. 8 – Illustration of mixing process with volumetric ratio of V_{org}:V_{aq} 1:1 and displacer r = 60 mm. Differential rotational speed constant at Δn = −175 rpm. Basic rotational speed of agitator increased by n_c = +800 rpm. Basic rotational speed: (A) n_c = 500 rpm, (B) n_c = 1300 rpm.

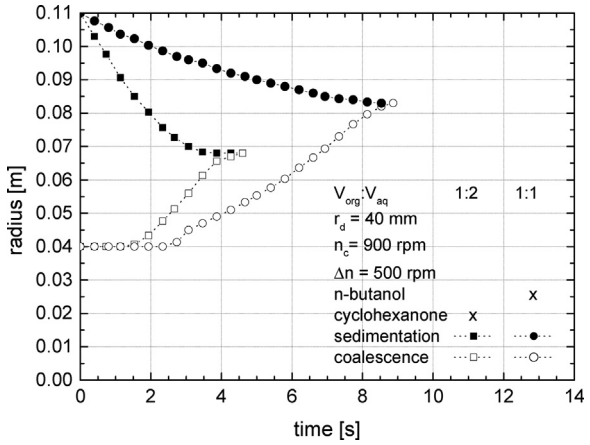

Fig. 9 – Results from SCBSC experiments (Δn = 500 rpm, n_c = 900 rpm and r_d = 40 mm). Filled symbols (■●) show the sedimentation and empty symbols (□○) the coalescence. Cycles (●○) show the *n*-butanol/water-system with V_{org}:V_{aq} 1:1 and squares (■□) show the cyclohexanone/water-system V_{org}:V_{aq} 1:2.

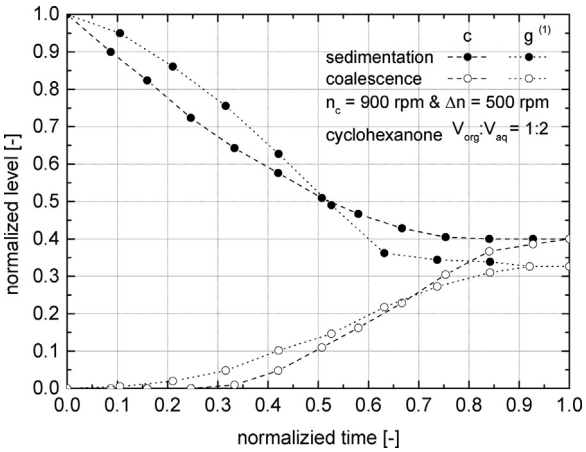

Fig. 10 – Normalized separation results from gravitational [(1)](Henschke, 1995) (dashed line) and from the SCBSC with Δn = 500 rpm and n_c = 900 rpm (dotted line) experiments for the cyclohexanone/water-system V_{org}:V_{aq} 1:2 system. Filled symbols (●) show the sedimentation and empty symbols (○) the coalescence.

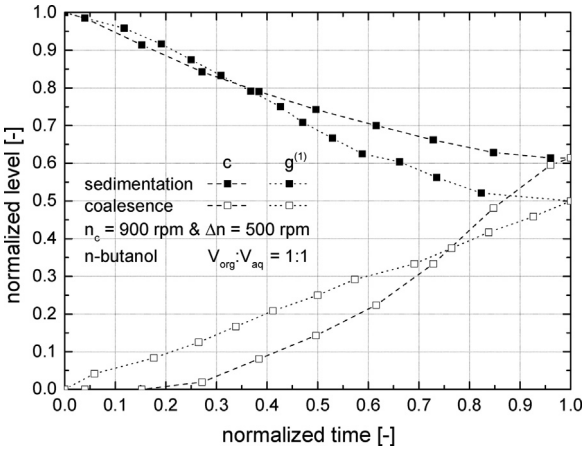

Fig. 11 – Normalized separation results from gravitational [(1)](Henschke, 1995) (dashed line) and from the SCBSC with Δn = 500 rpm and n_c = 900 rpm (dotted line). Experiments for *n*-butanol/water-system V_{org}:V_{aq} 1:1 system. Filled symbols (■) show the sedimentation and empty symbols (□) the coalescence.

Depending on basic rotation speed a minimal differential rotation is needed to mix the entire liquid–liquid system. To obtain comparable results while changing basic rotational speed the differential rotation needs to be sufficiently high enough, so that the centrifugal force field is relatively weaker compared to the turbulence field ($F_C = f(n_c) \ll F_T = f(\Delta n)$). Thus, the induced turbulence and its effect on droplet formation can be prevented by applying a higher centrifugal acceleration. Concluding that, the experimental set-up presents an attractive method for detailed investigation of the two phase mixing process and the contribution of the force field. For experimental results presented in this work a differential rotational speed of Δn = 500 rpm was chosen to ensure sufficient homogenization.

For an analysis of the centrifugal liquid–liquid separation two experimental results are depicted in Fig. 9. Both batch settling experiments are performed at a basic rotation of n_c = 900 rpm and a differential rotation of Δn = 500 rpm. With regard to the averaged acceleration (Eq. (3)), the applied centrifugal force field was 73 times higher compared to the gravitational field. The liquid–liquid system was dispersed at a phase ratio of 1:1 for *n*-butanol/water system and 1:2 for cyclohexanone/water system. The organic (lighter) phase was the dispersed phase. Thus, sedimentation is observed from the outer to the inner radius, opposite coalescence occurs from the inner to the outer radius.

To compare the overall separation behavior centrifugal batch as well as gravitational batch experiments are normalized as shown in Figs. 10 and 11. Gravity batch settling results are taken from Henschke (Henschke, 1995). For a better comparison, the experimental data from gravitational experiments are presented inverse to the real sedimentation directions. In both figures the ordinate axis represents the normalized level of the sedimentation and coalescence front and the abscissa axis represents the normalized process time. Measured values in the centrifugal field are shown as filled points with dashed lines and measured values from gravitational field as filled points with dotted lines. Form of the points represents in square the *n*-butanol and in circle the cyclohexanone system.

Table 3 – Dispersion Number for gravity and SCBSC experiments.

Disperse phase	Dispersion number N_{Di}		
	Gravitational	Centrifugal (n = 900 rpm)	Ratio
Cyclohexanone	0.00246	0.00220	1.11620
n-Butanol	0.00228	0.00110	2.07372

Sedimentation starts instantaneous after the ending of power input and earlier compared to coalescence, which starts delayed. Due to the radius dependent acceleration, sedimentation is faster at higher radius, which leads to an increase of dispersion hold-up before coalescence can start. The sedimentation behavior is characterized by a non-linear course, due to the reduction of the centrifugal force over the radius. Separation of cyclohexanone and water occurs faster than the separation of *n*-butanol and water, although the density difference of the cyclohexanone system is smaller. This is probably caused by a higher interfacial tension resulting in lager droplets which lead to a higher buoyancy force. Certainly, a large influence of the hold-up and thus the swarm behavior is also conceivable. It must be emphasized that in the centrifugal field the initial hold-up of droplets increase with decreasing radial position due to reduced acceleration acting on the droplets. The number of droplets is further elevated by particle motion on radial trajectories (Detloff and Lerche, 2008).

As shown in Figs. 10 and 11 the normalized sedimentation as well as coalescence curves are comparable regardless of the force field. Hence, the increase in sedimentation velocity is proportional to the coalescence progress. Thus, the overall separation behavior is not influenced by higher acceleration. Compared to gravitational force field the sedimentation within the centrifugal force field starts earlier, conversely the coalescence begins later. With progressing separation, the sedimentation and coalescence curves of both force fields cross each other. This can be explained by the centrifugal force field and the cylindrical design as mention before. Detloff describes similarly observations for the dilution of a suspension by increasing particle velocity and particle motion on radial trajectories. Their contribution points out that this effect is only characteristic for the sedimentation in the centrifugal field (Detloff and Lerche, 2008).

In Table 3 calculated dispersion numbers N_{Di} for the gravitational and centrifugal field as well as their ratios are given. In both cases, dispersion numbers for centrifugal acceleration, calculated by SCBSC data, are different in comparison to the dispersion number of gravitational acceleration, which are calculated from literature data. For the cyclohexanone/water system N_{Di} is 1.12 and for the *n*-butanol/water system 2.07 times higher compared to the batch settling experiments in gravitational force field. Thus, a direct transformation of results from gravitational field to centrifugal field is not possible. Since the determination of N_{Di} is not considering flow conditions a possible explanation are the different sedimentation velocity of the droplet swarm and the film drainage in centrifugal field compared to gravitational field.

4. Conclusion

This work deals with the characterization of liquid–liquid phase separation within the centrifugal field. A new standardized stirred centrifugal batch settling cell (SCBSC) is presented. A novel rotor–rotor/stator system is successfully applied for mixing and separating of two immiscible liquids within centrifugal field. To realize the mixing process the turbulence must be greater than the centrifugal force field. The mixing process itself requires a more detailed investigation to understand the influence of increasing rotational speed.

With the SCBSC, liquid–liquid separation behavior can be investigated in detail in dependence on centrifugal force field. Like in the gravitational field the separation in the SCBSC is characterized by a sedimentation curve and a coalescence curve as well as overall separation time. By normalization of the separation progress with regard to level and separation time, comparable overall separation behavior for test systems are shown. Small differences in sedimentation and coalescence can be explained by the centrifugal field and the radius dependent acceleration. Finally, the dimensionless dispersion number N_{Di} is calculated to compare the test results of gravitational and centrifugal separation investigation. The dispersion number N_{Di} for the centrifugal acceleration is higher than for the gravitational field. However, a prediction of the overall separation time t_E for enhanced centrifugal acceleration based on gravitational results are not possible by the use of the dispersion number. Hence, for the clarification and understanding of the physical basics, more extensive experimental investigation will be conducted. A detailed study of the swarm separation in centrifugal field will be part of further investigations. Thus, new swarm separation models for faster sedimentation velocities in centrifugal field are focused. The influence of different centrifugal acceleration on the separation time, the swarm influence as well as further test results of several liquid–liquid systems will be presented.

Notation

A	Agitator
B	Baffle
D	Displacer
C	Centrifugal cell
F	Force
F_C	Centrifugal force
F_T	Turbulence force
V	Volume
Z	Dispersion band thickness/separation path
a	Acceleration
b	Buoyancy
c	Centrifugal
d	Diameter
g	Gravitational
h	Height
h_0	Overall separation path way
h%	Normalized height
i	Inner
l	Length
m	Mass
n	Rotation
o	Outer
Δn	Differential rotation
q	Volume flow
r	Radius
t	Time
t_E	Overall separation time
t%	Normalized time
w	Wide
N_{Di}	Dispersion number

ω	Angular frequency
ρ	Density
η	Viscosity
σ	Interfacial tension

Abbreviations

SCBSC	Stirred centrifugal batch settling cell
ACC/ACE	Annular centrifugal contactor/extractor
rpm	Rounds per minute
org	Organic
aq	Aqueous

Acknowledgments

This work was performed as part of the Cluster of Excellence "Tailor-Made Fuels from Biomass", which is funded by the Excellence Initiative by the German federal and state governments to promote science and research at German universities. Further, the authors thank RWTH Aachen University — department 4.1 Technology Transfer for the assumption of the patent application.

Appendix A. Supplementary data

Supplementary data associated with this article can be found, in the online version, at http://dx.doi.org/10.1016/j.cherd.2017.09.005.

References

Arafat, H.A., Hash, M.C., Hebden, A.S., Leonard, R.A., 2001. Characterization and Recovery of Solvent Entrained During the Use of Centrifugal Contactors. Argonne, 30 pp.

Bernstein, G.J., Grosvenor, D.E., Lenc, J.F., Levitz, N.M., 1973. Development and Performance of a High-speed Annular Centrifugal Contactor. Chemical Enineering Division.

Bernstein, G.J., Leonard, R.A., Ziegler, A.A., Steindler, M.J., 1987. An improved annular centrifugal contactor for solvent extraction reprocessing of nuclear reactor fuel. In: 84th National Meeting, American Institute of Chemical Engineers.

Beveridge, T., 2000. Large-scale centrifugation. Handbook of Methods and Instrumentation in Separation Science, vol. 1. Academic Press Minister of Public Works and Government Services, Canada, pp. 320–329.

Birdwell, J.F., McFarlane, J., Hunt, R.D., Luo, H., DePaoli, D.W., Schuh, D.L., Dai, S., 2006. Separation of ionic liquid dispersions in centrifugal solvent extraction contactors. Sep. Sci. Technol. 41 (10), 2205–2223, http://dx.doi.org/10.1080/01496390600745719.

Brunner, A., 1985. Schwerölreinigung—Zentrifugalabscheider. Tech. Rundsch. Sulzer 4, 47–58.

Cambiella, A., Benito, J.M., Pazos, C., Coca, J., 2006. Centrifugal separation efficiency in the treatment of waste emulsified oils. Chem. Eng. Res. Des. 84 (1), 69–76, http://dx.doi.org/10.1205/cherd.05130.

Cao, S., Duan, W., Chengqian, W., 2013. Effects of structure parameters on the hydraulic performance of the ϕ20 annular centrifugal contactor. Energy Procedia 39, 461–466, http://dx.doi.org/10.1016/j.egypro.2013.07.237.

Detloff, T., Lerche, D., 2008. Centrifugal separation in tube and disc geometries: experiments and theoretical models. Acta Mech. 201 (1–4), 83–94, http://dx.doi.org/10.1007/s00707-008-0074-y.

Duan, W., Cao, S., 2015. Determination of the liquid hold-up volume and the interface radius of an annular centrifugal contactor using the liquid-fast-separation method. Chem. Eng. Commun. 203 (4), 548–556, http://dx.doi.org/10.1080/00986445.2015.1048802.

Duan, W., Cheng, Q., Zhou, X., Zhou, J., 2009. Development of a ϕ20 mm annular centrifugal contactor for the hot test of the total TRPO process. Prog. Nucl. Energy 51 (2), 313–318, http://dx.doi.org/10.1016/j.pnucene.2008.08.002.

Duan, W., Song, C., Wu, Q., Zhou, X., Zhou, J., 2005. Development and performance of a new annular centrifugal contactor for semi-industrial scale. Sep. Sci. Technol. 40 (9), 1871–1883, http://dx.doi.org/10.1081/SS-200064531.

Eggert, A., Bednarz, A., Sirbirtsev, S., Jupke, A., 2016. Vorrichtung und Verfahren zur Untersuchung des Phasentrennverhaltens von wenigstens zwei Phasen im Zentrifugalfeld (DE 102016002949.8).

Eggert, A., Sirbirtsev, S., Jupke, A., 2016. Vorrichtung und Verfahren zur Untersuchung und/oder Durchführung einer Reaktion von wenigsten zwei Phasen im Zentrifugalfeld (DE 102016012649.3).

Gebauer, K., Steiner, L., Hartland, S., 1982. Zentrifugalextraktion—Eine Literaturübersicht. Chem. Ing. Tech. 54 (5), 476–496, http://dx.doi.org/10.1002/cite.330540511.

Hemfort, H., 1983. Separatoren—Zentrifugen für Klärung, Trennung, Extraktion. GEA Westfalia Separator AG.

Henschke, M., 1995. Dimensionierung liegender Flüssig-flüssig-Abscheider anhand diskontinuierlicher Absetzversuche. Dissertation. Aachen, Technische Hochschule, VDI-Verlag, Düsseldorf, 161 pp.

Jammoal, Y., Lee, J., 2015. Drop velocity in a rotating liquid–liquid system. Chem. Eng. Res. Des. 104, 638–646, http://dx.doi.org/10.1016/j.cherd.2015.10.003.

Kadam, B.D., Joshi, J.B., Koganti, S.B., Patil, R.N., 2008. Hydrodynamic and mass transfer characteristics of annular centrifugal extractors. Chem. Eng. Res. Des. 86 (3), 233–244, http://dx.doi.org/10.1016/j.cherd.2007.10.020.

Kadam, B.D., Joshi, J.B., Koganti, S.B., Patil, R.N., 2009. Dispersed phase hold-up, effective interfacial area and Sauter mean drop diameter in annular centrifugal extractors. Chem. Eng. Res. Des. 87 (10), 1379–1389, http://dx.doi.org/10.1016/j.cherd.2009.03.005.

Klasson, K.T., Taylor, P.A., Walker, J.F., Jones, S.A., Cummins, R.L., Richardson, S.A., 2005. Modification of a centrifugal separator for in-well oil–water separation. Sep. Sci. Technol. 40 (1–3), 453–462, http://dx.doi.org/10.1081/SS-200042503.

Krebs, T., Schroën, C., Boom, R.M., 2012. Separation kinetics of an oil-in-water emulsion under enhanced gravity. Chem. Eng. Sci. 71, 118–125, http://dx.doi.org/10.1016/j.ces.2011.10.057.

Leonard, R.A., 1988. Recent advances in centrifugal contactor design. Sep. Sci. Technol. 23 (12–13), 1473–1487, http://dx.doi.org/10.1080/01496398808075643.

Leonard, R.A., 1995. Solvent characterization using the dispersion number. Sep. Sci. Technol. 30 (7–9), 1103–1122, http://dx.doi.org/10.1080/01496399508010335.

Leonard, R.A., Bernstein, G.J., Pelto, R.H., Ziegler, A.A., 1981. Liquid–liquid dispersion in turbulent couette flow. AIChE J. 27 (3), 495–503, http://dx.doi.org/10.1002/aic.690270320.

Leonard, R.A., Bernstein, G.J., Ziegler, A.A., Pelto, R.H., 2006. Annular centrifugal contactors for solvent extraction. Sep. Sci. Technol. 15 (4), 925–943, http://dx.doi.org/10.1080/01496398008076278.

Leonard, R.A., Chamberlain, D.B., Conner, C., 1997. Centrifugal contactors for laboratory-scale solvent extraction test. Sep. Sci. Technol. 32 (1–4), 193–210, http://dx.doi.org/10.1080/01496399708003194.

Leonard, R.A., Regalbuto, M.C., Aase, S.B., Arafat, H.A., Falkenberg, J.R., 2001. Hydraulic performance of a 5 cm contactor four caustic-side solvent extraction, Chemical Technology Division, Argonne National Laboratory, Argonne, Illinois, United States Department of Energy under Contract W-31-109-Eng-38 – ANL-02/18.

Li, S., Duan, W., Chen, J., Wang, J., 2012. CFD simulation of gas–liquid–liquid three-phase flow in an annular centrifugal contactor. Ind. Eng. Chem. Res. 51 (34), 11245–11253, http://dx.doi.org/10.1021/ie300821t.

Mandal, K., Kumar, S., Vijayakumar, V., Mudali, U.K., Ravisankar, A., Natarajan, R., 2015. Hydrodynamic and mass transfer

studies of 125 mm centrifugal extractor with 30% TBP/nitric acid system. Prog. Nucl. Energy 85, 1–10, http://dx.doi.org/10.1016/j.pnucene.2015.05.005.
Meikrantz, D.H., Laq, J.D., Todd, T.A., 2005. Design attributes and scale up testing of annular centrifugal contactors. Chemical Engineering Division of the AIChE National Meeting (INL/CON-05-00088).
Meikrantz, D.H., Macaluso, L.L., Flim, W.D., Heald, C.J., Mendoza, G., Meikrantz, S.B., 2002. A new annular centrifugal contactor for pharmaceutical processes. Chem. Eng. Commun. 189, 1629–1639, http://dx.doi.org/10.1080/00986440290123633.
Meikrantz, D.H., Meikrantz, S.B., Macaluso, L.L., 2001. Annular centrifugal contactors for multiple stage extraction processes. Chem. Eng. Commun. 188 (1), 115–127, http://dx.doi.org/10.1080/00986440108912900.
Otillinger, F., 1988. Fluiddynamik und Stoffübergang in Zentrifugalextraktoren, Technische Universität München, Germany, 46 pp.
Padial-Collins, N.T., Zhang, D.Z., Zou, Q., Ma, X., VanderHeyden, W.B., 2006. Centrifugal contactors: separation of an aqueous and an organic stream in the rotor zone (LA-UR-05-7800). Sep. Sci. Technol. 41 (6), 1001–1023, http://dx.doi.org/10.1080/01496390600641611.
Patra, J., Pandey, N.K., Muduli, U.K., Natarajan, R., Joshi, J.B., 2013. Hydrodynamic study of flow in the rotor region of annular centrifugal contactors using CFD simulation. Chem. Eng. Commun. 200 (4), 471–493, http://dx.doi.org/10.1080/00986445.2012.706838.
Plat, R., 1994. Gravitational and Centrifugal Oil–water Separators, Thesis Technical University Delft, Netherlands, 168 pp.
ReinholdSchilp_1982_Fluiddynamik_in Zentrifugal-Extraktoren I.
Rivalier, P., Gandi, F., Duhamet, J., 2004. Development of new annular centrifugal solvent extractioncontactor, Poster P1-48, at ATLANTE 2004, Nimes, France online: IAEA International Atomic Enery Agency https://www.iaea.org/.
Rousselet Robatel. Scale-up of Liquid/Liquid Centrifuges, Manufacturing centrifuges and centrifugal extraction equipment, whitepaper, brochures from Robatel online www.rousselet-robatel.com.
Schaflinger, U., 1990. Centrifugal separation of a mixture. Fluid Dyn. Res. 6 (6), 213–249, http://dx.doi.org/10.1016/0169-5983(90)90014-P.
Schilp, R., 1983. Fluiddynamik in Zentrifugalextraktoren. IDEA-Verlag GmbH Puchheim, 318 pp.
Schilp, R., Blaß, E., 1982. Fluiddynamik in Zentrifugalextraktoren. Chem. Ing. Tech. 54 (4), MS 990/1982.
Schilp, R., Blaß, E., 1983. Bewegung und Stabilität von Tropfen in nichtmischbaren Flässigkeiten bei hohen Zentrifugalfeldstßrken. Chem. Ing. Tech. 55 (8), MS 1133/83.
Simon, E., 1982. Die diskontinuierliche Zentrifuge als Betriebssystem in der Chemischen Industrie. Chem. Ing. Tech. 54 (4), 333–350, http://dx.doi.org/10.1002/cite.330540408.
Stölting, M., 1979. Bildung und Bewegung von Einzeltopfen in einer rotierenden Flüssigkeit, Theses Technical University Munich, Germany, 83 pp.
Stölting, M., Blaß, E., 1978. Tropfenbildung und Tropfenbewegung in einem rotierenden Extraktor. Chem. Ing. Tech. 50 (6), MS 595/78.
Stölting, M., Hengstler, N., Blaß, E., 1979. Auslegung von Zentrifugalextraktoren—Eine Verbsindung von verfahrenstechnischen und physikochemischen Problemstellungen. Ber. Bundesgesellschaft Phys. Chem. 83 (11), 1116–1120, http://dx.doi.org/10.1002/bbpc.19790831115.
Svn Ayyappa, Balamurugan, M., Kumar, S., Mudali, U.K., Natarajan, R., 2014. Hydrodynamic and Mass Transfer Studies in 50 mm Centrifugal Extractor, Seminar on Recent Advances in Fuel Cycle Technologies, Kalpakkam, India, 4 pp.
van Kemenade, E., Brouwers, B., van Benthum, R., 2014. Centrifugal separation with emphasis on the rotational particle separator. ChemBioEng Rev. 1 (6), 262–272, http://dx.doi.org/10.1002/cben.201400027.
Vedantam, S., Joshi, J.B., 2006. Annular centrifugal contactors—a review. Chem. Eng. Res. Des. 84 (7), 522–542, http://dx.doi.org/10.1205/cherd.05219.
Vedantam, S., Wardle, K.E., Tamhane, T.V., Ranade, V.V., Joshi, J.B., 2012. CFD simulation of annular centrifugal extractors. Int. J. Chem. Eng. 2012 (94), 1–31, http://dx.doi.org/10.1155/2012/759397.
Wardle, K.E., Allen, T.R., Swaney, R., 2009. CFD simulation of the separation zone of an annular centrifugal contactor. Sep. Sci. Technol. 44 (3), 517–542, http://dx.doi.org/10.1080/01496390802634398.
Webster, D.S., Jennings, A.S., Kishbaugh, A.A., Bethmann, H.K., 1967. Performance of Centrifugal Mixer-Settler in the Repricessing of Nuclear Fuel, Symposium on Recent Advances in Reprocessing of Irradiated Fuel American Institute of Chemical Engineers Meeting New York, New York 20 pp.